

AL/CF-TP-1994-0006

AD-A277 920



ARMSTRONG  
LABORATORY

EVALUATION OF PULSED DOPPLER  
BUBBLE DETECTION

Hegeon Kwun  
W.D. Jolly  
D.G. Alcazar

Southwest Research Institute  
6220 Culebra Road  
San Antonio, TX 78284

CREW SYSTEMS DIRECTORATE  
CREW TECHNOLOGY DIVISION  
2504 D Dr, Suite 1  
Brooks Air Force Base, TX 78235-5104

DTIC  
ELECTE  
APR 07 1994  
S E D

March 1994

Final Technical Paper for Period 1 October 1988 - 30 September 1989

Approved for public release; distribution is unlimited.

4488 94-10530



94 4 6 0 59

DTIC QUALITY INSPECTED 3

AIR FORCE MATERIEL COMMAND  
BROOKS AIR FORCE BASE, TEXAS

## NOTICES

This technical paper is published as received and has not been edited by the technical editing staff of the Armstrong Laboratory.

When Government drawings, specifications, or other data are used for any purpose other than in connection with a definitely Government-related procurement, the United States Government incurs no responsibility or any obligation whatsoever. The fact that the Government may have formulated or in any way supplied the said drawings, specifications, or other data, is not to be regarded by implication, or otherwise in any manner construed, as licensing the holder, or any other person or corporation; or as conveying any rights or permission to manufacture, use, or sell any patented invention that may in any way be related thereto.

The Office of Public Affairs has reviewed this paper, and it is releasable to the National Technical Information Service, where it will be available to the general public, including foreign nationals.

This paper has been reviewed and is approved for publication.



Andrew A. Pilmanis, Ph.D.  
Chief, High Altitude Protection Function



F. Wesley Baumgardner, Ph.D.  
Chief, Systems Research Branch



Ronald C. Hill, Colonel, USAF, BSC  
Chief, Crew Technology Division

# REPORT DOCUMENTATION PAGE

Form Approved  
OMB No. 0704-0188

Public reporting burden for this collection of information is estimated to average 1 hour per response, including the time for reviewing instructions, searching existing data sources, gathering and maintaining the data needed, and completing and reviewing the collection of information. Send comments regarding this burden estimate or any other aspect of this collection of information, including suggestions for reducing this burden, to Washington Headquarters Services, Directorate for Information Operations and Reports, 1215 Jefferson Davis Highway, Suite 1204, Arlington, VA 22202-4302, and to the Office of Management and Budget, Paperwork Reduction Project (0704-0188), Washington, DC 20503.

1. AGENCY USE ONLY (Leave blank)		2. REPORT DATE March 1994	3. REPORT TYPE AND DATES COVERED Final - 1 October 1988 - 30 September 1989		
4. TITLE AND SUBTITLE Evaluation of Pulsed Doppler Bubble Detection			5. FUNDING NUMBERS C - FQ7624-89-000001 PE - 61101F PR - 7930 TA - 18 WU - 9A		
6. AUTHOR(S) Hegeon Kwun W.D. Jolly D.G. Alcazar					
7. PERFORMING ORGANIZATION NAME(S) AND ADDRESS(ES) Southwest Research Institute 6220 Culebra Road San Antonio, TX 78284			8. PERFORMING ORGANIZATION REPORT NUMBER		
9. SPONSORING/MONITORING AGENCY NAMES(S) AND ADDRESS(ES) Armstrong Laboratory (AFMC) Crews Systems Directorate Crew Technology Division 2504 D Drive Ste 1 Brooks Air Force Base, TX 78235-5104			10. SPONSORING/MONITORING AGENCY REPORT NUMBER AL/CF-TP-1994-0006		
11. SUPPLEMENTARY NOTES  Armstrong Laboratory Technical Monitor: Andrew A. Pilmanis, (210) 536-3545					
12a. DISTRIBUTION/AVAILABILITY STATEMENT  Approved for public release; distribution is unlimited.			12b. DISTRIBUTION CODE		
13. ABSTRACT (Maximum 200 words)  The High Altitude Protection Function of the Crew Technology Division has used a portable Doppler array to monitor venous gas emboli in human research subjects exposed to reduced high altitudes. The existing Doppler equipment was limited in that subjects were required to maintain a specific body position to achieve consistent bubble grade analysis, especially during exercise. It was surmised that engineering modifications might resolve the dilemma. The target frequency and sound wave pulses were to be modified to maintain focus on the precordium allowing for continuous tracking of bubble sounds. A prototype, pulsed-wave, Doppler bubble detection instrument with transducers was designed and developed. This system demonstrated greater depth of penetration and the ability to localize the interrogation area; however, altitude simulation tests revealed the prototype to be unsatisfactory due to the high level of noise generated internally by the CW Doppler circuitry. Recommendations were made of redesign, but development was not pursued due to funding limitations. Also, Doppler echoimaging was found to provide equal if not better analysis of bubble grades with the addition of visual cues to ensure accurate placement and timely monitoring regardless of physical activity.					
14. SUBJECT TERMS Bubble grades Bubble sounds Bubbles			Doppler Doppler systems		15. NUMBER OF PAGES 50
					16. PRICE CODE
17. SECURITY CLASSIFICATION OF REPORT Unclassified	18. SECURITY CLASSIFICATION OF THIS PAGE Unclassified	19. SECURITY CLASSIFICATION OF ABSTRACT Unclassified	20. LIMITATION OF ABSTRACT UL		

## TABLE OF CONTENTS

	<u>Page</u>
<b>LIST OF FIGURES</b> .....	v
<b>LIST OF TABLES</b> .....	v
<b>1. INTRODUCTION</b> .....	1
<b>1.1 Background and Objective</b> .....	1
<b>1.2 Project Work Effort</b> .....	2
<b>1.2.1 Phase I - Development and Evaluation of Pulsed Bubble                 Detection Instrument</b> .....	2
<b>1.2.2 Phase II - Evaluation of Remote Control Methods</b> .....	2
<b>1.3 Roadmap of Final Report</b> .....	3
<b>1.4 Summary of Accomplishments and Findings</b> .....	3
<b>2. DEVELOPMENT OF PROTOTYPE PULSED DOPPLER INSTRUMENT</b> .....	6
<b>2.1 Ultrasonic Safety and Power Measurement</b> .....	6
<b>2.1.1 Safety Standard</b> .....	6
<b>2.1.2 Ultrasonic Power Measurement</b> .....	6
<b>2.2 Design and Development of Prototype Pulsed Doppler Instrument</b> .....	7
<b>2.2.1 Design Criteria and Selection of Required Electrical                 Performance Characteristics</b> .....	7
<b>2.2.2 Prototype Pulsed Doppler Instrument</b> .....	10
<b>3. PRELIMINARY EVALUATION OF PROTOTYPE PULSED DOPPLER INSTRUMENT</b> .....	13
<b>3.1 Laboratory Evaluation</b> .....	13
<b>3.2 Evaluation on Human Subjects</b> .....	17
<b>4. ADDITIONAL MODIFICATIONS OF PROTOTYPE PULSED DOPPLER INSTRUMENT</b> .....	19
<b>4.1 Time-Controlled Gain Modification</b> .....	19
<b>4.2 Results of Reevaluation on Human Subjects</b> .....	19
<b>5. SUMMARY AND RECOMMENDATIONS</b> .....	21
<b>5.1 Summary</b> .....	21
<b>5.2 Recommendations</b> .....	21

TABLE OF CONTENTS (CONT'D)

	Page
6. REFERENCES .....	23
APPENDIX A - MEASUREMENT OF ULTRASONIC POWER USING A REACTION RADIATION-FORCE BALANCE .....	25
APPENDIX B - CIRCUIT DESCRIPTION AND SCHEMATICS .....	35

Accession For	
NTIS CRA&I	<input checked="" type="checkbox"/>
DTIC TAB	<input type="checkbox"/>
Unannounced	<input type="checkbox"/>
Justification .....	
By .....	
Distribution/	
Availability Codes	
Dist	Avail and/or Special
A-1	

## LIST OF FIGURES

<u>Figure</u>		<u>Page</u>
1	Photograph of prototype instrument along with the sensor array developed in the previous project and two individual transducers fabricated in this project .....	4
2	Frequency response of Doppler shift due to bubble velocity in pulmonary artery of subject during decompression using IAPM 1032G 5-MHz Doppler bubble detector .....	8
3	Block diagram of the prototype pulsed Doppler bubble detector instrument .....	11
4	Schematic of bubble simulator set up for evaluation of the pulsed Doppler instrument .....	13
5	Example of ultrasonic signals and the gate signal for selecting sensing area displayed on an oscilloscope .....	15
6	Examples of Doppler signals detected at various gate positions: at 70 (top), 75 (middle), and 80 (bottom) microseconds .....	16
7	Illustration of the sharpness of the time resolution of the gated receiver and the pulsed oscillator .....	17

## LIST OF TABLES

<u>Table</u>		<u>Page</u>
1	Intensity Ranges Produced by Current Ultrasound Systems .....	7
2	Power Limited Pulse-Voltage Combinations .....	9

## 1. INTRODUCTION

### 1.1 Background and Objective

The U.S. Air Force has lost pilots as a result of rapid air decompression in the cockpit at high altitudes. This loss of pressure causes dissolved nitrogen in the bloodstream to form bubbles that, in turn, reach the capillaries in the brain and cause pilot blackout. If the pilot does not recover, both the aircraft and pilot are destroyed.

One long-standing research program at the High Altitude Simulation Facility of Brooks AFB School of Aerospace Medicine (SAM) has been directed toward developing a remote monitor that could (1) detect the initial formation of decompression-induced bubbles and (2) evaluate methods of controlling or counteracting the tendency to produce unconsciousness. The most recent SAM monitoring technique under study uses an ultrasonic beam to detect nitrogen bubbles passing through the heart. Detection is based on the Doppler shift of the reflection from the moving bubbles.

In a previous project under the SAM's decompression sickness program, Southwest Research Institute (SwRI) developed an ultrasonic transducer array which could be switched remotely (1). The switchable array was used to steer the beam into the optimum location in the heart to monitor the initiation of decompression bubbles in a physically active subject. The present project was directed toward correcting a problem encountered in the previous project; that is, deep-chested individuals could not be monitored during exercise with existing instruments. It was assumed that the ultrasonic beam was too weak to convey the Doppler shifted bubble signal to the operator.

There are two possible ways of increasing penetration depth of the ultrasonic beam waves: either by lowering the frequency or by increasing power. A lower frequency wave is attenuated less and, thus, penetrates farther. One shortcoming of lowering the frequency, however, is that the detectability of small-size bubbles is reduced because of the longer wavelength. A higher power wave will penetrate deeper before it is attenuated to the undetectable level without compromising the detectability of small bubbles, but the continuous irradiation of high-power ultrasonic waves has a potentially harmful biological side effect.

One solution for overcoming these shortcomings and still achieving a greater penetration depth is to use pulsed ultrasonic waves instead of continuous waves. To achieve this greater depth without increasing the average power, a pulse with a larger amplitude can be used. Also, the detectability of small bubbles would not be compromised if the ultrasonic frequency were unchanged. Furthermore, the pulsed Doppler bubble detection would allow localization of the position of interrogation by time gating the received signals from the right ventricle; this, in turn, would improve the signal-to-noise (S/N) ratio by minimizing the effects of stray signals from other reflectors.

The objective of the project described in this report was, therefore, to modify an IAPM 1032G continuous-wave Doppler bubble-detector instrument existing at Brooks AFB for operation as a pulsed Doppler bubble-detection instrument. The modified instrument would use the steerable-beam transducer array developed under the previous program. The performance and capability of the modified instrument would be evaluated in the Brooks Altitude Chamber by the client.

## 1.2 Project Work Effort

The following phases and tasks were identified in SwRI Proposal 17-7242 to accomplish the project goals.

### 1.2.1 Phase I - Development and Evaluation of Pulsed Bubble Detection Instrument

- *Task 1 - Development of a Prototype Instrument*

A prototype instrument was to be developed by modifying the existing USAFSAM Doppler bubble detector which operated on continuous ultrasonic waves. Factors to be considered included the maximum allowable average ultrasonic power (in conformance with the Safety Standard for Diagnostic Ultrasound Equipment, American Institute of Ultrasound in Medicine/ National Electrical Manufacturers Association Standard Publication No. UL1-1981), pulse amplitude, pulse length, repetition rate of the pulse, and the highest Doppler frequency shift detectable without aliasing.

- *Task 2 - Laboratory Evaluation*

The developed prototype instrument was to be evaluated in the laboratory. A pair of ultrasonic probes were to be fabricated for use with the prototype instrument. The same probe design used for the switchable transducer array developed in the previous program was to be utilized. The average ultrasonic power output was to be measured to ensure that the output was under the maximum allowable limit. Sensitivity, bubble detectability, and ability to localize the interrogation area was to be determined by inducing bubbles in water to simulate bubbles in a blood flow.

- *Task 3 - Preliminary Evaluation on Human Subjects*

The prototype instrument and probes were to be evaluated on human subjects at USAFSAM, Brooks AFB, by USAFSAM personnel. Areas which require further improvement were to be identified, and suitable adjustments or changes were to be made to the system.

- *Task 4 - Final Evaluation on Human Subjects*

The improved system was to be evaluated on human subjects at USAFSAM by USAFSAM personnel. The capability and limitation of the system including the depth penetration, sensitivity, and detectability of bubbles were to be determined. Specific recommendations were to be made for subsequent development and implementation of the system as a research tool as well as a field instrument for routine bubble monitoring.

### 1.2.2 Phase II - Evaluation of Remote Control Methods

In anticipation of the need for a remote control to follow heart movements during exercise periods, methods of remote control were to be evaluated. These methods included remote switching of ultrasonic array and remote control of gate depth/position. If the remaining funding of the program allowed, a prototype device was to be designed, tested, and demonstrated at USAFSAM.

Note: Owing to problems encountered in Phase I, time and funds were not available for Phase II.

### 1.3 Roadmap of Final Report

This final report covers the evaluation of safety standards on ultrasonic power limitation for exposure of living tissue, the development of a pulsating blood-flow and bubble simulator, the invention of a radiation force balance method for measurement of radiated power from ultrasonic transducers (Appendix A), a description of the development and evaluation of the pulsed Doppler prototype instrument, a detailed circuit description of the instrument (Appendix B), a chronological description of the prototype instrument development (Appendix C), and recommendations for tasks leading to successful operation of the instrument.

### 1.4 Summary of Accomplishments and Findings

A prototype, pulsed, Doppler bubble-detection instrument was designed and developed. Figure 1 shows a photograph of the prototype instrument along with the sensor array developed in the previous project and two individual transducers fabricated in this project. The development of the prototype was accomplished by adding the following circuits to an existing continuous-wave (CW) Doppler instrument used in the previous project (1):

- Pulsing circuits to produce a tone burst pulse
- RF power amplifier to increase the amplitude of the pulse
- Timing and gating circuits to allow gating of the received signal at an arbitrary depth
- Sample-and-hold (S&H) and filters to produce audible Doppler signals
- Time-controlled gain (TCG) circuits to compensate for the attenuation of signal with depth.

The developed system did demonstrate the greater depth of penetration (approximately 10 cm) and the ability to localize the interrogation area. However, because of a relatively high level of noise which was internally generated from the IAPM 1032G CW Doppler circuit, the system lacked adequate S/N ratio for bubble detection, particularly in deep-chested subjects. As a result, altitude simulation tests on human subjects were not satisfactory.

In order to improve the S/N ratio of the developed system to a satisfactory level, the circuit adapted from the IAPM 1032G Doppler instrument needed to be redesigned or replaced. This task was beyond the funding constraints of the subject project. However, specific recommendations on ways for improving the prototype pulsed Doppler instrument were identified for consideration in a follow-on developmental project.

During the course of the altitude simulation tests on human subjects, it was found that the depth of the interrogation area for Doppler bubble detection in heavy-chested subjects was no more than approximately 8 to 9 cm. The difficulties in Doppler bubble monitoring on deep-chested subjects encountered previously with the existing CW instrument were believed, therefore, to be due to the strong reflected signals from other nearby targets, which swamped feeble bubble signals. Once the S/N ratio of the prototype pulsed Doppler instrument has been improved through redesigning of circuits, the instrument is expected to be capable of monitoring bubbles in deep-chested subjects.

In addition to the development of the pulsed Doppler instrument, a new technique of measuring ultrasonic power, which was named "Reaction Radiation-Force Balance," was developed

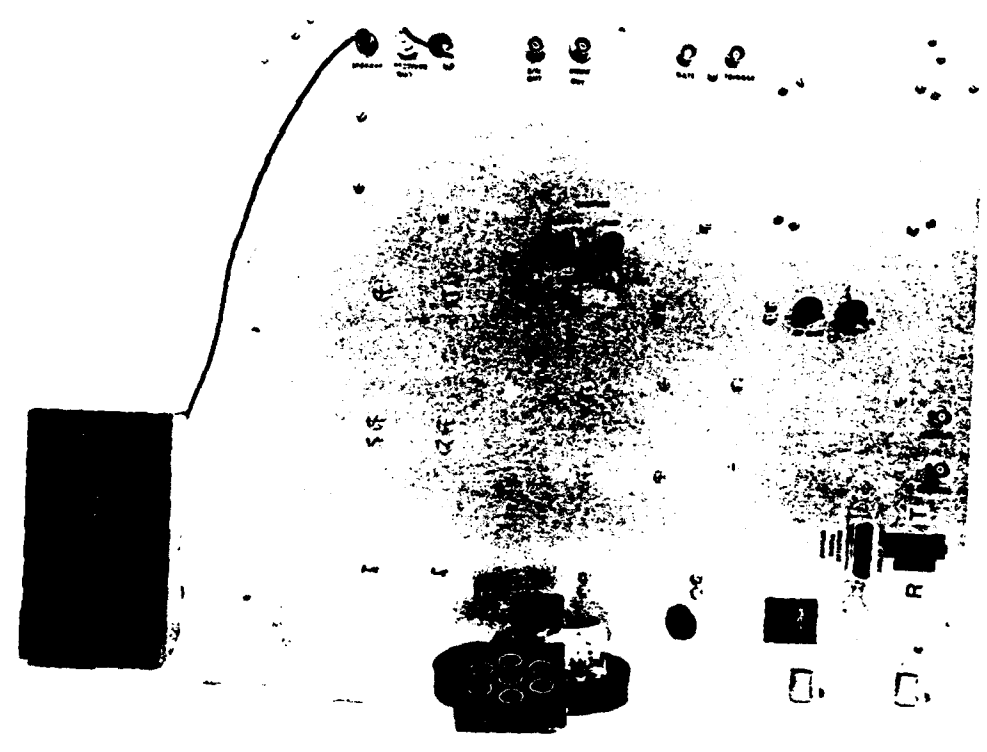
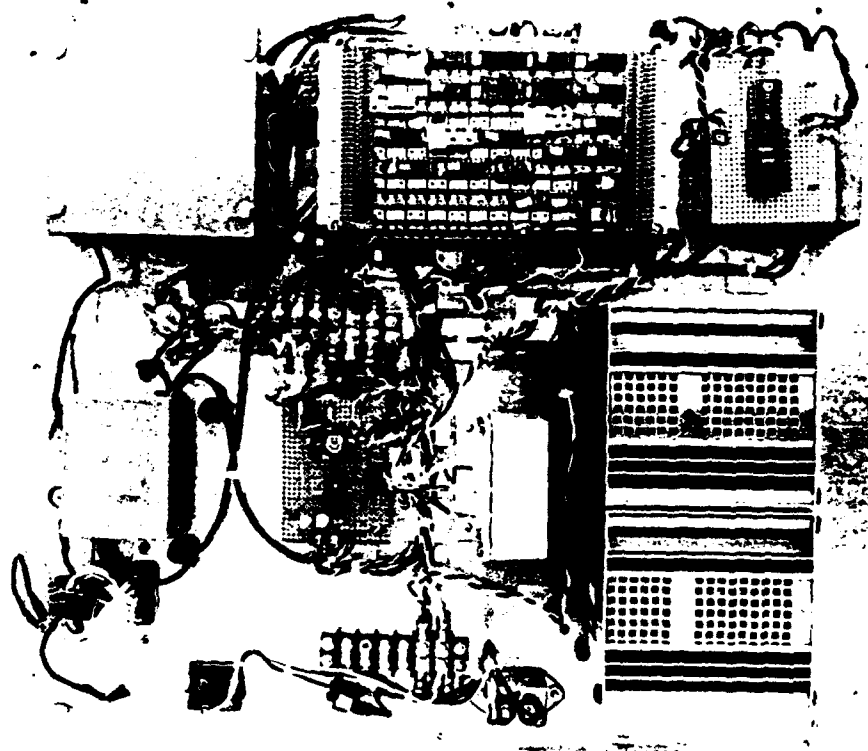


Figure 1. Photograph of prototype instrument along with the sensor array developed in the previous project and two individual transducers fabricated in this project

in this project (Appendix A). The reaction force experienced by a transducer upon emission of ultrasonic waves is measured by using a mechanical balance, and the associated acoustic power output may be calculated. This innovative technique is unique, and a patent is being pursued by SwRI for SAM for the technique.

Also, a blood flow simulator with injected bubbles was designed and fabricated. The simulator was a useful tool for bench testing the pulsed Doppler bubble detector.

## 2. DEVELOPMENT OF PROTOTYPE PULSED DOPPLER INSTRUMENT

### 2.1 Ultrasonic Safety and Power Measurement

#### 2.1.1 Safety Standard

The general ultrasonic safety guidelines given in AIUM/NEMA Safety Standard for Diagnostic Ultrasound Equipment (2) recommends the use of minimum practical acoustic intensity levels and exposure time. No quantitative guidelines are given, however, because of imprecise knowledge of any potential hazard to humans based upon current experimental and epidemiological studies. Nevertheless, according to the above standard, there have been, as of October 1978, no confirmed significant biological effects in mammalian tissues reported from exposures to intensities below  $100 \text{ mW/cm}^2$  (intensity referred to here is spatial peak, temporal average as measured in free field in water at near-far field transition distance of the transducer). Furthermore, for ultrasonic exposure times less than 500 seconds and greater than 1 second, such effects have not been demonstrated even at higher intensities when the product of intensity and exposure time is less than 50 joules/cm<sup>2</sup>.

As a reference, the ranges of intensities produced by current diagnostic ultrasonic systems reported in the above standard are given in Table 1.

#### 2.1.2 Ultrasonic Power Measurement

Ultrasonic power can be measured by using various methods including radiation force and calorimetry. The above AIUM/NEMA Safety Standard for Diagnostic Ultrasound Equipment recommends the use of radiation force or calibration methods; the latter simply means to use a calibrated transducer whose power has been determined by other direct method such as radiation force or calorimetry.

Presently known direct power measurement methods require an elaborate instrumentation system. Since setting up such a system was beyond the scope of the project, a simpler way of measuring power was sought. This effort led to development of a new technique for measuring radiation force named "Reaction Radiation-Force Balance." The technique measures the total ultrasonic power produced by a transducer operated in a CW mode by measuring the reaction force due to the transmitted ultrasonic beam. A detailed description of the technique and experimental arrangement to implement the technique are given in Appendix A.

Using the reaction radiation force balance technique, the total ultrasonic power produced by a single-element, 3/8-inch-diameter, 5-MHz transducer (shown in Figure 1) was measured. The transducer was specially fabricated for the project by using a 5-MHz, 9.5-mm-diameter, lead metaniobate piezoelectric crystal. The transducer was of the same design as the individual elements of the sensor array (also shown in Figure 1), but had an epoxy layer matched for water load. The transducer was, therefore, approximately 3 dB more efficient than the array sensor elements. The total power produced by the transducer at 20 V, peak-to-peak, applied voltage, CW excitation, was approximately 186 mW. The area of the 9.5-mm-diameter transducer was  $0.71 \text{ cm}^2$ , giving a power density of  $262 \text{ mW/cm}^2$  at the transducer face in water. Adjustment of the duty factor would be needed to maintain the average power limit of  $100 \text{ mW/cm}^2$  while maximizing the instantaneous power to achieve the desired depth of penetration.

Table 1

## INTENSITY RANGES PRODUCED BY CURRENT ULTRASOUND SYSTEMS

Type of Equipment	Spatial Average-- Temporal Average Intensity on the Radiating Surface (mW/cm <sub>2</sub> )	Spatial Peak-- Temporal Average Intensity (mW/cm <sub>2</sub> )	Spatial Peak-- Pulse Average Intensity (W/cm <sub>2</sub> )
Static Pulse Echo Scanners and M Mode Equipment	0.4-202	10-200	0.5-280
Automatic Sector Scanners (Phased Arrays and Wobblers)	2.7-60	45-200*	25-100
Sequenced Linear Arrays	0.06-10	0.1-12	25-100
Pulsed Doppler, Primarily for Cardiac Work	3-32	50-290	3-14
Doppler Instruments, Primarily for Obstetric Applications	3-25	Spatial Peak Intensity 9-75	
Continuous Wave Doppler, Primarily for Peripheral Vascular	38-840	110-2500**	

\*This value was measured with the scanning mechanism arrested for M mode and at the maximum system pulse repetition rate.

\*\*Estimate based on the spatial average--temporal average.

## 2.2 Design and Development of Prototype Pulsed Doppler Instrument

### 2.2.1 Design Criteria and Selection of Required Electrical Performance Characteristics

The aim of this design was to achieve 12.7-cm penetration depth into the human chest within the limit of the maximum allowable ultrasonic power. The upper bound for the pulse repetition rate, the pulse width, and the transmitted pulse voltage required of the prototype pulsed Doppler instrument was selected as follows.

*Repetition Rate* - The desired penetration depth of the instrument was up to 12.7 cm (5 inches). In order to detect bubbles up to this range, the signals reflected from the bubbles at the maximum depth must be allowed to reach the receiving transducer before the next pulse is transmitted. Using the velocity of sound in soft tissue of approximately  $1.5 \times 10^5$  cm/sec, the round-

trip time of the wave to a 12.7-cm depth is 169 microseconds. The corresponding pulse repetition frequency (prf) allowed is  $5.92 \times 10^3$  per second. This means that the maximum measurable Doppler frequency shift is 2.96 kHz if the Nyquist criterion is observed. The Doppler frequency shift,  $dF$ , is given as

$$dF = 2 F_0 v \cos Q / c \quad (1)$$

where  $F_0$  is the frequency of ultrasonic wave,  $c$  is the velocity of ultrasonic wave in soft tissues,  $v$  is the velocity of the reflector (i.e., bubbles), and  $Q$  is the angle between the ultrasonic beam and blood flow directions. With the ultrasonic frequency of 5 MHz and an angle of 60 degrees, the above 2.96-kHz frequency shift corresponds to a bubble velocity of approximately 89 cm/sec.

Experimental measurement of the Doppler frequency range was made by evaluating the Doppler frequency of bubble signals recorded from the IAPM 1032G Doppler instrument in CW mode operation. Analysis of actual bubble sounds recorded during altitude chamber experiments at Brooks by Dr. J. D. Adams showed that the 1032G recorded a Doppler frequency shift of up to 3000 Hz, as shown in Figure 2.

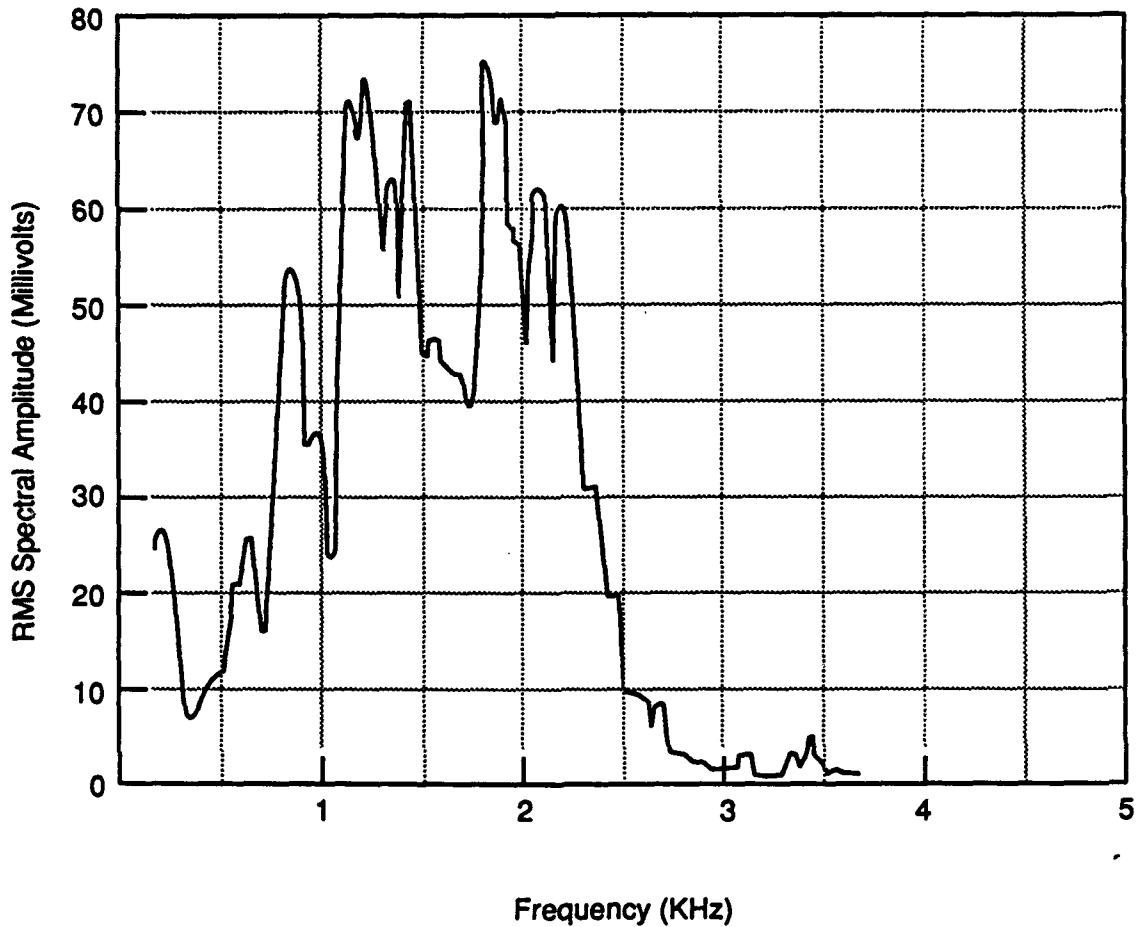


Figure 2. Frequency response of Doppler shift due to bubble velocity in pulmonary artery of subject during decompression using IAPM 1032G 5-MHz Doppler bubble detector

Figure 2 shows the spectrum of Doppler frequency from recorded bubble sounds played back on a Sharp RD 670 AV cassette recorder/player. The RD 670 AV with frequency response to 10,000 Hz did not limit the frequency response of the recorded bubble sounds. The measured frequency shift from bubbles agrees well with the theoretically predicted Doppler shift for a beam of angle of 60 degrees to the direction of bubble flow.

The duration (or width) of the pulse determines the length of the sample volume in which the Doppler bubble signals are monitored. The sample length, SL, is given as

$$SL = c d / 2 \tag{2}$$

where d is the pulse duration (Pd). Larger sample lengths make the detection of bubbles easier but make the identification of location difficult. If a Pd of 10 microseconds is used, the corresponding sample length is approximately 0.75 cm. The Pd is an adjustable parameter within the allowable maximum ultrasonic power of 100 mW/cm<sup>2</sup>.

Maximum ultrasonic power of 100 mW/cm<sup>2</sup> was selected as the upper limit because it is comparable to the power output of current diagnostic ultrasonic systems shown in Table 1 and is believed to be safe. The total ultrasonic power output of the transducer was measured by the reaction radiation force balance technique described in Appendix A. Total ultrasonic attenuation in soft tissue is 5 dB/cm. The actual ultrasonic intensity in the target area, i.e., the heart, will be substantially lower (at a depth of 8 cm, by more than 40 dB).

*Pulse Repetition (prf) Frequency* - Frequency of 6000 pulses/sec was chosen to give a depth range of up to 12.5 cm in human tissue and a maximum detectable Doppler frequency shift of 3 kHz. As mentioned in Section 2.1.2, the 5-MHz transducer fabricated in this project produced approximately 186 mW total power at 20 V, peak-to-peak applied voltage in CW excitation. Since the cross section of the transducer was approximately 0.71 cm<sup>2</sup>, the corresponding power intensity was approximately 262 mW/cm<sup>2</sup>. The ultrasonic power is proportional to the square of the applied voltage. Therefore, for the 100 mW/cm<sup>2</sup> power intensity, the peak-to-peak applied voltage in CW excitation should be approximately 20 V x (100/262)<sup>1/2</sup> = 12.4 V.

In pulsed excitation, the maximum peak-to-peak applied voltage can be increased substantially without increasing overall temporal average power. How much it can be increased is dependent on prf and Pd. If the pulse produced is square in shape, the increasing factor is given as (prf x Pd)<sup>-1/2</sup>.

Using prf = 6000 pulses/sec, the allowable peak-to-peak applied voltage for various pulse widths is as follows:

Table 2

POWER LIMITED PULSE-VOLTAGE COMBINATIONS

<u>Pd (in microsec)</u>	<u>Voltage P/P (in V)</u>
1.0	160
2.5	101
5.0	72
7.5	58
10.0	51

The prototype pulsed Doppler instrument was designed to have an adjustable applied voltage of up to 100 V peak-to-peak and adjustable pulse duration of up to 10 microseconds.

For bubble detection through human tissue, the penetration depth of the IAPM 1032G Doppler instrument used in the previous project (1) was estimated by Dr. Adams at about 7.5 cm. The instrument applies approximately 4.85 volts, peak-to-peak, to the transducer.

The 50 volts, peak-to-peak, to be generated by the pulsed Doppler unit will increase the peak ultrasonic intensity by

$$10 \log (50/4.85)^2 = 20 \text{ dB.}$$

The attenuation coefficient in soft tissue at 5 MHz is about 5 dB/cm of distance or 10 dB/cm of range (round trip). The increased peak intensity due to pulsed wave operation of 20 dB, therefore, adds 2 cm to the range of the IAPM 1032G. With the pulsed Doppler unit, therefore, the penetration depth will be improved to about 9.5 cm. Using this information, we modified the Institute of Applied Physiology and Medicine (IAPM) 1032G Doppler bubble detector to perform pulsed Doppler measurement of frequencies up to 3000 Hz.

### 2.2.2 *Prototype Pulsed Doppler Instrument*

The Doppler bubble detector instrument used at Brooks was the Institute of Applied Physiology and Medicine (IAPM) 1032G, a 5-MHz, CW ultrasonic instrument (3). The model 1032G is an adaptation of a Doppler detector first developed in 1971. The technical specification of the instrument electronics is tabulated below.

<b>Power:</b>	6 rechargeable NiCd Batteries, CF15T	
<b>Transmitter:</b>	<b>Output:</b>	4-6 volts, peak-to-peak, 50-ohm load
	<b>Frequency:</b>	Approximately 5 MHz, determined by crystal
<b>Receiver:</b>	<b>Input impedance:</b>	50 ohms
	<b>Recorder output</b>	10k ohms
	<b>Headphone output:</b>	8 ohms impedance, drives any standard headphones
	<b>Sensitivity:</b>	0.033-mm bubbles

This instrument was used in the previous project (1) without modification of the electronics. For the purpose of converting to a pulsed Doppler operation, some modification was needed.

The instrument's CW oscillator was caused to emit ultrasonic pulses to the transmitting transducer by an analog switch which connected the transmitter to the transducer for a period of 10 microsec every 1/6000 sec. The received signal was inhibited from the audio output except when the sample/hold acquired a new signal from the receiver circuit output. The receiver gate was synchronized with the transmitter gate and delayed by an adjustable interval equal to the time required for the transmitted pulse to return from the monitored chamber of the heart. The gated, pulsed Doppler process not only allows the use of higher peak power for greater penetration but also allows the high-amplitude, near-surface Doppler signal to be rejected. Rejection of the near-surface Doppler permits higher receiver gain for detection of the bubble signals. A block diagram of the prototype Doppler detector instrument is shown in Figure 3. A complete circuit description of the instrument is provided in Appendix B.

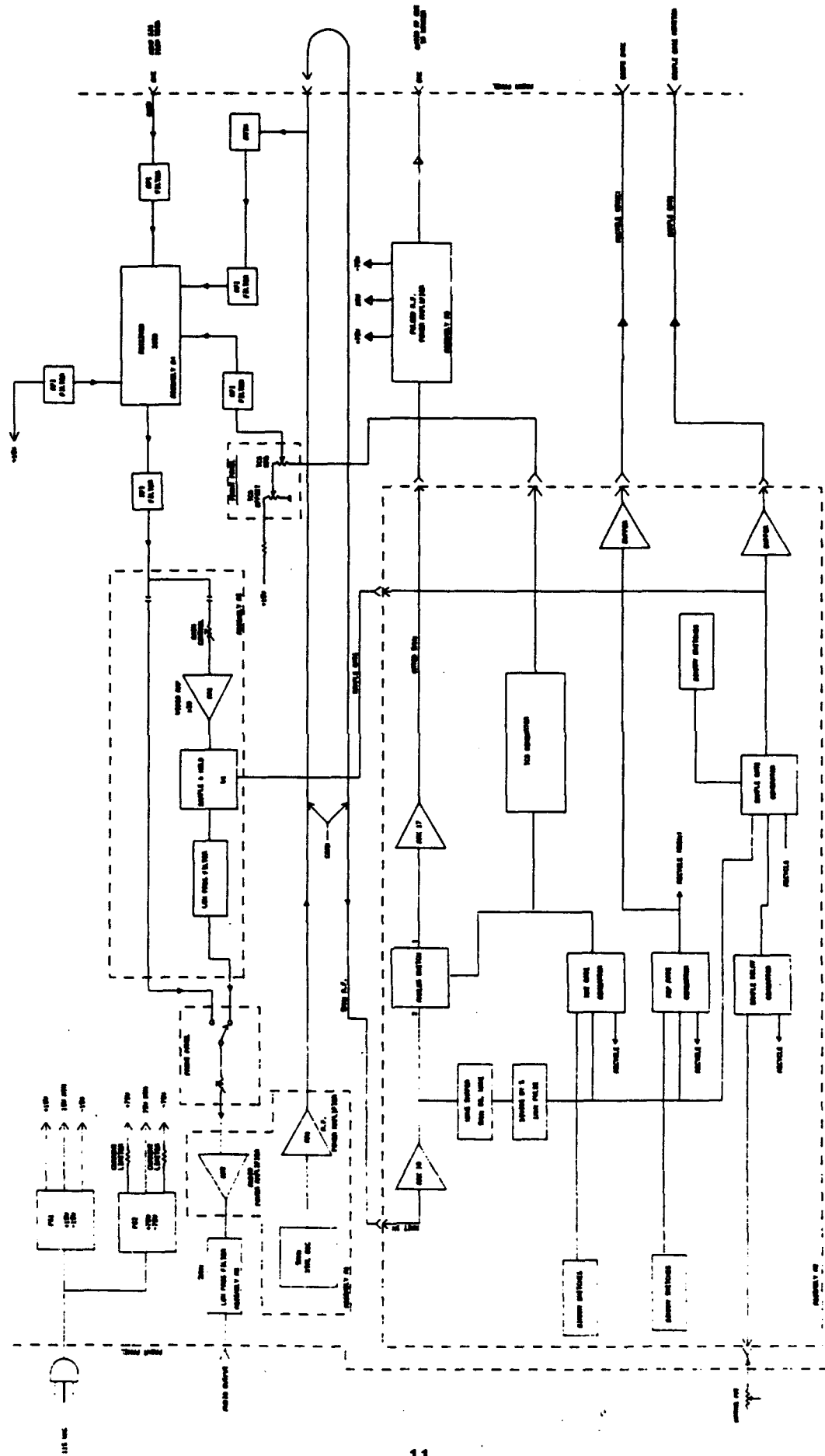


Figure 3. Block diagram of the prototype pulsed Doppler bubble detector instrument

Preliminary testing of the first prototype instrument revealed that a strong noise corresponding to the prf of the instrument was present. An attempt to reduce this noise to an acceptable level using an analog filter was not highly successful. To overcome the problem, a sample-and-hold (S/H) circuit was subsequently incorporated into the system.

### 3. PRELIMINARY EVALUATION OF PROTOTYPE PULSED DOPPLER INSTRUMENT

#### 3.1 Laboratory Evaluation

The first version of the prototype was evaluated in the laboratory. To facilitate the evaluation, a blood-flow simulator was designed and fabricated. The simulator consisted of a container for fluid such as water, mechanical fixture for holding the ultrasonic transducer, and hydraulic pump and hoses for pulsating fluid circulation. Figure 4 shows a schematic diagram of the

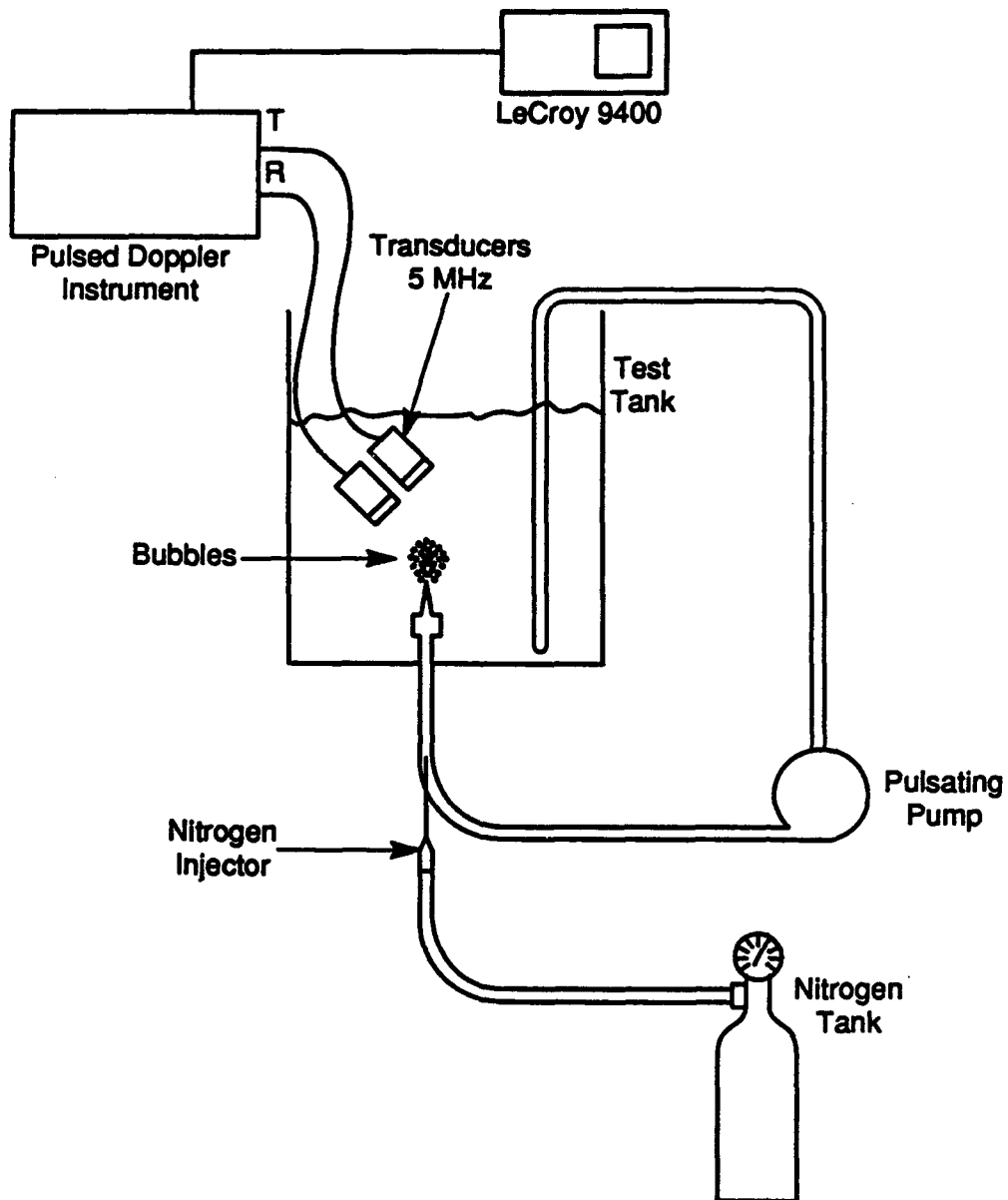


Figure 4. Schematic of bubble simulator set up for evaluation of the pulsed Doppler instrument

simulator. The fluid was circulated from the top, through the pulsating hydraulic pump, and to the bottom of the container where the fluid was injected back to the container through an opening with a rubber check valve. Pulsation rate was variable up to 60 pulsations/sec.

Initially, a jelly-type fluid substance mixed with air was used and circulated. Due to the viscosity of the fluid, the trapped air bubbles remained in the fluid without rising to the surface and were easily circulated. The prototype instrument produced strong Doppler signals from these bubbles demonstrating that pulsed Doppler detection works well. The air bubbles entrapped were in various sizes, from very tiny to 3 to 4 mm. The Doppler bubble signal amplitudes varied too much from one measurement to another. Thus, a meaningful evaluation of the instrument was difficult to achieve with this arrangement.

As an alternative to the jelly-type fluid, water was used. Because of the buoyancy of air bubbles in water, the bubbles rise to the top and form air pockets in the circulation loop. Thus, the air bubbles in water could not be circulated. An arrangement schematically described in Figure 4 was used. Air bubbles were injected into the circulation loop near the opening at the bottom of the container using a hypodermic needle. The air was supplied using a pressurized nitrogen gas tank. The amount of air bubbles injected was adjusted by regulating the air pressure. The injected air bubbles discharged into the container with each pulsation of the hydraulic pump. The Doppler signals produced from these rising bubbles were detected and used for evaluation of the prototype instrument.

Figure 5 shows an example of ultrasonic signals and the gate signal for selecting sensing area displayed on an oscilloscope (Le Croy Model 9400, Dual 125-MHz Digital Oscilloscope). The upper figure shows two ultrasonic pulses separated by approximately 160 microseconds, and the envelope detected ultrasonic echoes reflected from air bubbles in between. The lower figure shows the gate signal which was positioned at approximately 97 microseconds from the preceding ultrasonic pulse. As shown in the upper figure, the ultrasonic pulse envelope was triangular rather than square in shape when the instrument was loaded with an ultrasonic transducer.

With the arrangement illustrated in Figure 4, Doppler signals from air bubbles in the pulsating flow were monitored while the distance between the transducer and the bubble injection valve were varied. Because of the very low attenuation in water (approximately 0.05 dB/cm at 5 MHz), Doppler signals of a high S/N ratio were observed throughout the entire depth range of the prototype instrument which was 12 cm.

The ability of localizing the sensing area by time-gating was evaluated. The transducers were placed at a distance of approximately 6 cm from the bubble injection valve in the bottom of the simulator. While varying the position of the gate, whose width was 5 microseconds, the resulting Doppler signals from the prototype instrument were recorded on an oscilloscope. Figure 6 shows examples of the Doppler signals detected using the Le Croy Model 9400 digital oscilloscope; the data shown in the figure were obtained with the gate position at 70, 75, and 80 microseconds, respectively.

To compare the Doppler signals obtained at various gate positions, the energy contained in the signal was calculated by integrating the square of the Doppler signal with time. In acoustic emission, the energy thus calculated is widely used as a measure of the strength of the event, and the same approach is adopted here. The calculation of the energy was done using the built-in data processing capability of the Le Croy digital oscilloscope. Figure 6 shows the energy of Doppler signal plotted as a function of the gate position. As shown, the response of the instrument dropped sharply when the gate was moved out of the 80-microsecond position which is the round-trip time of the ultrasonic wave over 6-cm distance. The data shown in Figure 7 clearly indicate the ability to localize the sensing area by time gating.

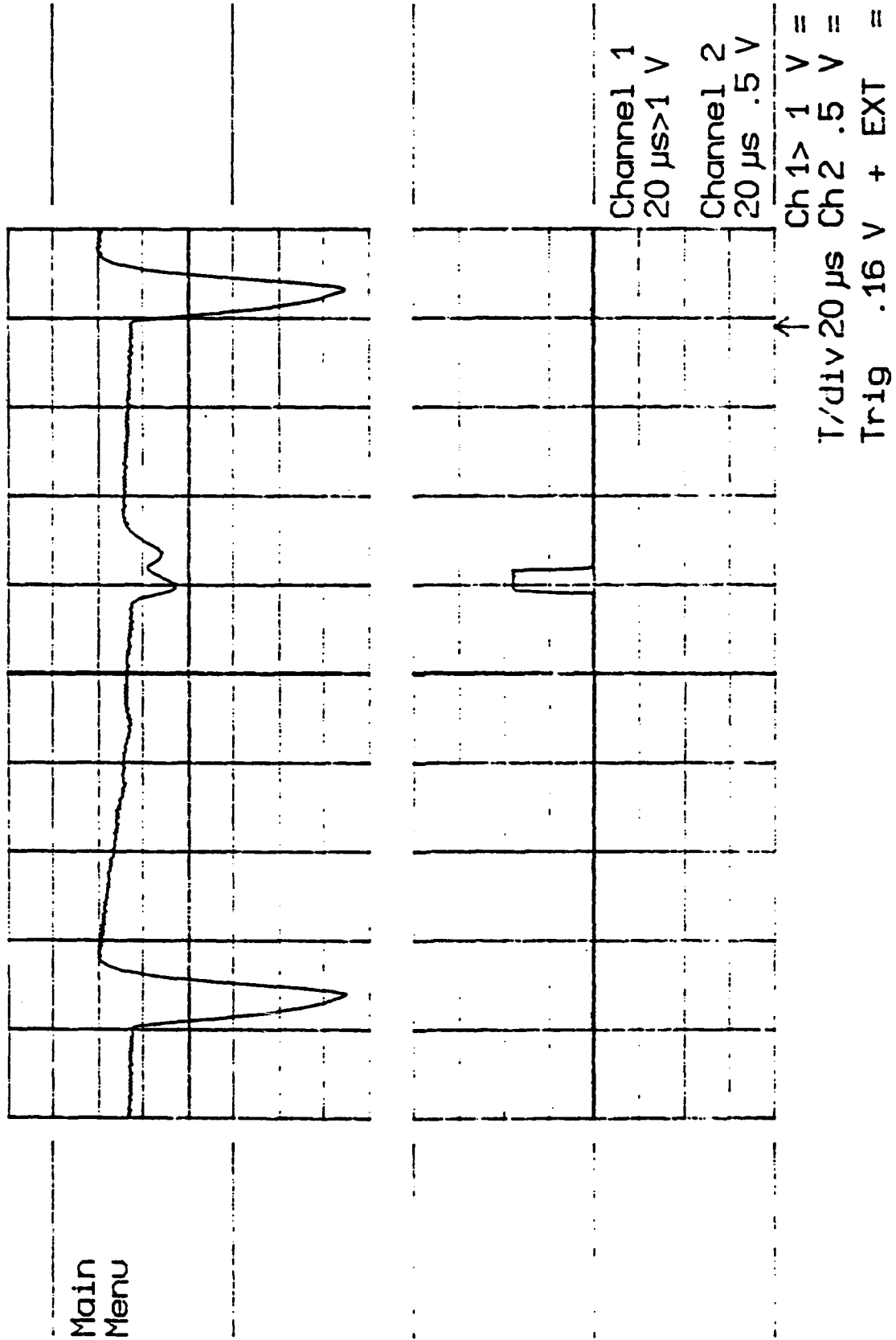


Figure 5. Example of ultrasonic signals and the gate signal for selecting sensing area displayed on an oscilloscope

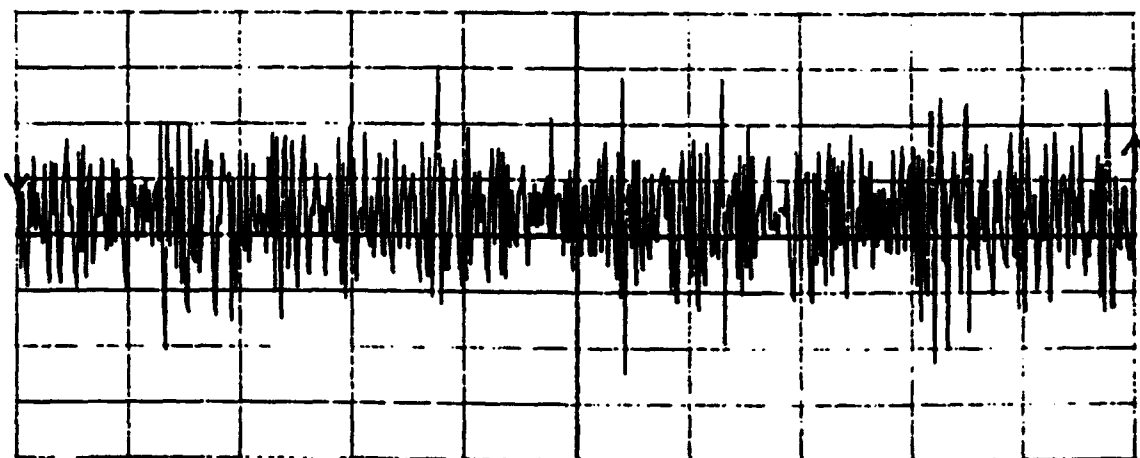
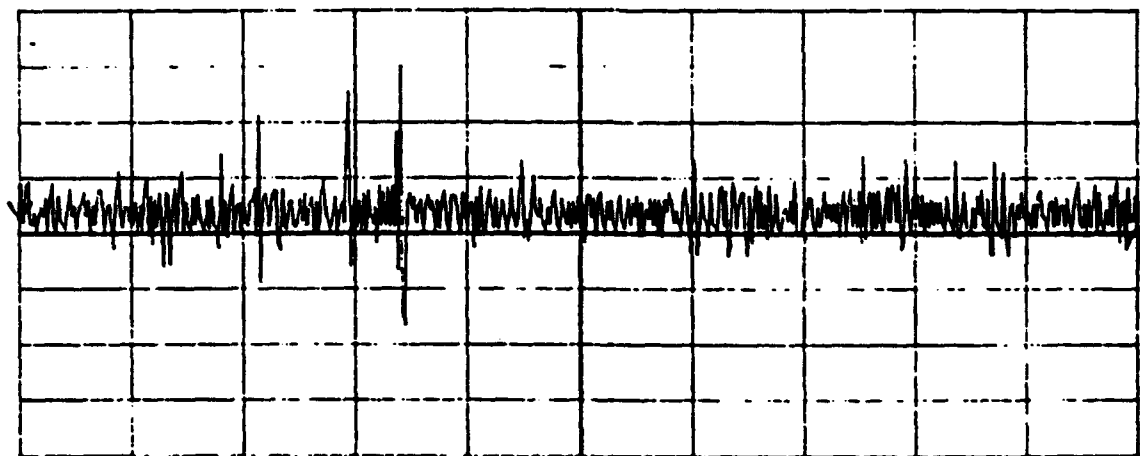
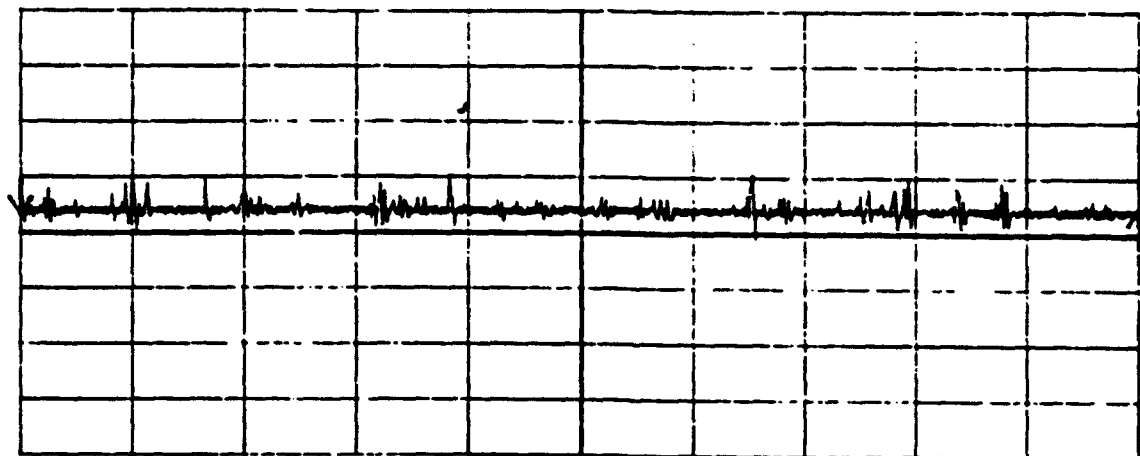


Figure 6. Examples of Doppler signals detected at various gate positions: at 70 (top), 75 (middle), and 80 (bottom) microseconds. X-axis - 0.5 sec/div, Y-axis - 0.2 V/div.

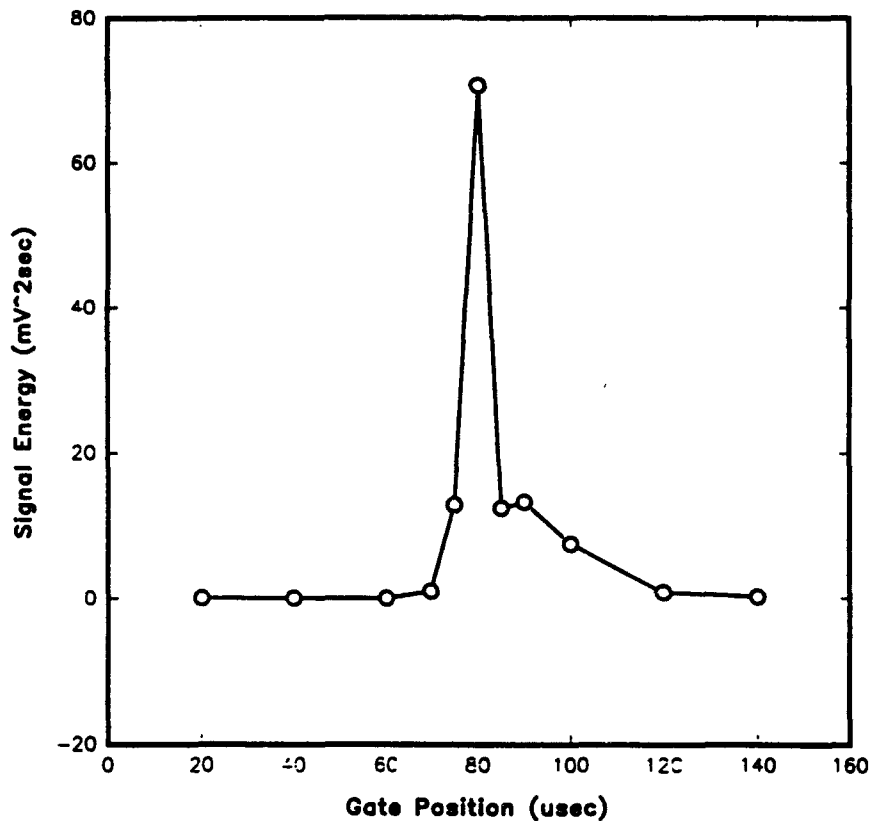


Figure 7. Illustration of the sharpness of the time resolution of the gated receiver and the pulsed oscillator. The depth resolution represented by the response peak was about 0.75 cm.

### 3.2 Evaluation on Human Subjects

Preliminary evaluation of the prototype pulsed Doppler instrument on human subjects was conducted at the Altitude Simulation Chamber Facility of the Brooks AFB during a period in late January of 1990. Tests were conducted on several subjects having medium to heavy chest sizes. Some subjects were put into a flight simulation and bubble formation in the blood was monitored intermittently for a period of a few minutes during the flight simulation. Both the prototype instrument and the Hewlett Packard ultrasonic instrument at Brooks were used for monitoring the Doppler bubble sounds.

The ultrasonic signals detected with the prototype instrument typically showed a large reflected signal at around 45- to 60-mm depth (60 to 80 microseconds after the initial pulse), along with some other signals of considerably lower amplitude occurring at a later time. In some cases, ultrasonic signals appeared at around 75- to 90-mm depth (100 to 120 microseconds). The Doppler sound from these late-arriving signals did not contain the landmark chirping sound from the tricuspid valve of the right ventricle. The late arriving signals were later identified as reflections from the backwall of the heart. When the gate was adjusted for less depth and set to the trailing edge of the large reflected signal occurring at about 60 TO 80 microseconds, the landmark heart valve sound was detectable with difficulty amidst a loud squeak at the prf. The preliminary testing on human subjects thus revealed unexpected problems which would require circuit improvements before Doppler bubble sounds could be monitored using the prototype instrument.

During the course of the altitude simulation tests, it was found from the B-scan display of the HP Heart Monitor Instrument that the depth of the area for monitoring Doppler bubble sounds was typically only about 50 to 70 mm; and, even for heavy-chested subjects, the depth was no more than approximately 80 to 90 mm. Based on the above observation, it was apparent that the difficulties encountered previously with the 1032G CW instrument on heavy-chested subjects must have been caused by the strong reflected signals from near-surface reflectors which swamped feeble bubble signals.

As for the modified 1032G prototype pulsed instrument, the large signals occurring at around 60 to 80 microseconds were exceeding the limit of the input voltage to the receiver section of the instrument. It was determined that the receiver recovered from the overload too slowly to permit the detection of Doppler signals from a depth region just beyond the region that gave rise to the overload. To operate the prototype instrument from 50- to 90-mm range, it was deemed necessary to incorporate time-controlled gain (TCG) in the circuit.

The TCG would provide a low initial gain which increased with time so that the near-surface reflected signal would be reduced to less than the input voltage limit of the receiver, and the signals occurring at a later time would be sufficiently amplified.

## 4. ADDITIONAL MODIFICATIONS OF PROTOTYPE PULSED DOPPLER INSTRUMENT

### 4.1 Time-Controlled Gain Modification

The TCG circuit was designed, installed, tested, modified, and retested. The receiver was then tested to measure effects of TCG operation on bandpass characteristic. No detrimental effect was found.

Clamping diodes were added at the output of the detector circuit to improve the recovery of the receiver following the transmitted tone burst. Also, capacitors were changed in order to limit the dc level shift at the output.

### 4.2 Results of Reevaluation on Human Subjects

Tests on human subjects to evaluate the effect of the TCG and other circuit modifications were conducted by Captain Gordon at Brooks AFB. Blood rush signals were detected in three different people, but still there was too much noise.

It was learned that the TCG action had the undesired effect of varying the level of the Doppler demodulation reference signal as well as the receiver gain. Doppler detection in the IAPM 1032G was accomplished by beating the received signal with a leakage signal coupled by stray capacitance from the system's 5-MHz crystal oscillator into the first stage of the receiver's rf amplifier. To prevent the TCG from affecting the reference signal level, steps were taken to reduce the leakage signal and to inject a controlled level of reference signal at a later stage in the rf amplifier that is not affected by the TCG signal.

The evaluation showed that the signal-to-noise ratio (SNR) was too low to permit bubble detection. The reason for this deficiency was not known, but there was some concern that the SNR might be degraded by the presence of objectionable stray electronic signals being generated and/or coupled as a result of the lengthy connections between the various modules. Therefore, work aimed at eliminating such noise was performed in an attempt to improve operation.

The steps taken to reduce the leakage of the 5-MHz signal and other noise-generating signals in the receiver consisted in placing rf filters in series with every signal circuit and power circuit leading into or out of the receiver. In every case, this consisted of winding the circuit pair for several turns around a ferrite core of toroidal shape. Using this technique, the receiver noise without the injected reference was not significantly greater than that specified for the circuit elements used.

These "cleanup" steps did not yield sufficient improvement. Work had to stop at this point and the cause of the low SNR is still unknown, but it is suggested that the following causes be evaluated if further work is performed:

- (1) It is possible that the noise is caused by an unusually high level of phase modulation noise in the 5.2-MHz local oscillator. This possibility could explain the observation that the amplitude of the noise in the receiver output is substantially reduced when the reference signal is removed from the receiver mixer. This symptom indicates that the noise might be caused by either (a) an unusually broad spectrum from the crystal oscillator or (b) the operation of the receiver mixer is unusually sensitive to amplitude modulation caused by the small, unavoidable noise present in any amplifier.

The next two possibilities are related to the circumstance that the net ultrasonic signal can be comprised of (a) the relatively weak-strength, but high-Doppler frequency, signals from blood flow and bubbler versus (b) the relatively strong, but low-Doppler frequency, signals from tissue movement accompanying heartbeat. If the net signal does have these two components, then it is possible that the poor detectability of bubbles could be caused by either or both of the following effects:

- (2) The strong, low-frequency signals could dominate the sense of hearing and thereby mask the bubble signals. Should this be the case, then considerable improvement could be obtained by using a high-pass filter to block the undesired low-frequency signals.
- (3) The low-frequency signals might be large enough to exceed the dynamic range of successful mixing needed to detect bubbles. Should this occur, then bubble signals might be present in only a small fraction of the heartbeat cycle. In this case, further degradation might be caused by audible "noise" generated by the nonlinearity occurring as the dynamic range is exceeded.

Should this phenomenon actually exist, then an effective improvement would be to employ a new receiver design which offered a greater dynamic range for Doppler detection.

The system was closed up and bench tested using a live subject. Blood rush sounds were detected though the system noise was still bothersome.

## 5. SUMMARY AND RECOMMENDATIONS

### 5.1 Summary

A prototype, pulsed, Doppler bubble detection instrument was designed and developed by adding the following circuits to an existing continuous wave (CW) Doppler instrument used in the previous project (1):

- Pulsing circuits to produce a tone burst pulse
- RF power amplifier to increase the amplitude of the pulse
- Timing and gating circuits to allow gating of the received signal at an arbitrary depth
- Sample-and-hold (S&H) and filters to produce audible Doppler signals
- Time-controlled gain (TCG) circuits to compensate for the attenuation of signal with depth and to enable the avoidance of receiver overload and subsequent slow recovery.

The developed system did demonstrate the greater depth of penetration (approximately 10 cm) and the ability to localize the interrogation area. However, because of a relatively high level of noise which was internally generated from the CW Doppler circuit retained, the system lacked adequate S/N ratio for Doppler bubble monitoring, particularly in heavy-chested subjects. As a result, satisfactory altitude simulation tests of the developed system could not be performed.

### 5.2 Recommendations

- (1) The goal of using pulsed Doppler ultrasound to detect gas bubbles at relatively large range is judged to be achievable. It is suspected that the failure to achieve that goal is due to inadequate performance of the receiver and/or local oscillator used.
- (2) The important functional characteristics in a receiver are:
  - Maintaining good FM detection over a large dynamic range of signal levels (at least 50-dB dynamic range).
  - Rapid recovery from overload caused by large signals preceding the range selected for bubble detection. It is recommended that the receiver be based on differential amplifiers exhibiting symmetrical limiting and that special care be used to eliminate the adverse effects of stored charges deposited on innerstage coupling capacitors as a result of limiting. If these principles are used, then it will not be necessary to use TCG.
- (3) The output of the frequency detector and the sample-and-hold circuit should be bandpass filtered to remove signals below about 300 Hz and to attenuate frequencies above the Nyquist frequency by more than 60 dB.
- (4) It may be very important to choose the receiver gain to be as low as practical for detecting bubble signals. Favoring low gain will help avoid the degrading effects of nonlinear operation as a result of high signal level.
- (5) If the intersection angle between the blood velocity vector and the ultrasonic beam is smaller than about 50 degrees, then the peak Doppler frequency will exceed the Nyquist

frequency (for 5-MHz operation) and it will be impossible to perceive bubble signals anywhere over the complete heartbeat cycle. (Low-velocity bubbles could be detected, but not high-velocity bubbles.) If this circumstance proves to be a problem, then it would be appropriate to reduce the operating frequency to around 2 MHz.

- (6) Reevaluate required depth of penetration and adjust rep-rate to maximum allowed by new required depth.
- (7) Tune output of power amplifier to operating frequency to reduce harmonics in output waveform.
- (9) Evaluate the phase noise of the local oscillator and make improvements, if necessary.

## 6. REFERENCES

1. H. Kwun, W. D. Jolly, and J. D. Adams, "Laboratory Prototype Switchable Ultrasonic Doppler Bubble Detector," Final Report, SwRI Project No. 17-1084, USAF Contract No. F33615-83-D-0602-0023, Subcontract No. L600034 (1987).
2. Safety Standard for Diagnostic Ultrasound Equipment, American Institute of Ultrasound in Medicine/National Electrical Manufacturers Association, Standards Publication No. UL 1-1981.
3. *Users Instructions, 1032G Bubble Detector.* Seattle, Washington: Institute of Applied Physiology and Medicine.

**APPENDIX A**  
**MEASUREMENT OF ULTRASONIC POWER USING**  
**A REACTION RADIATION-FORCE BALANCE**

## **MEASUREMENT OF ULTRASONIC POWER USING A REACTION RADIATION-FORCE BALANCE**

**H. Kwun, W. D. Jolly, and D. G. Alcazar  
Southwest Research Institute  
6220 Culebra Road  
San Antonio, Texas 78228-0510**

### **ABSTRACT**

A technique for measuring the total power output of an ultrasonic transducer using a reaction radiation-force balance is described. In this technique, the radiation force of an ultrasonic beam transmitted by a transducer is measured with a mechanical balance by weighing the reaction force exerted to the transducer. Compared with conventional radiation-force measurement techniques using a target, the technique is simpler and more accurate.

### **INTRODUCTION**

Measurements of the ultrasonic power from medical ultrasonic devices are important in studying physical and biological effects of ultrasound as well as in determining the safety of the device. Techniques for measuring absolute ultrasonic power, therefore, have received extensive attention. Those most commonly used are calorimetry and radiation force (1,2).

With the calorimetry techniques, the ultrasonic energy is converted into heat by absorbing it in a liquid medium. The resulting rise of medium temperature is measured to determine the ultrasonic power. The power can be calculated analytically if thermal characteristics of the calorimeter including heat capacity and the rate of heat loss to the surroundings are known. Typically, however, the ultrasonic power is determined using a calibration curve established with a known amount of electrical heat input. While simple to use, these techniques require an elaborate system to achieve good accuracy.

With the radiation-force techniques, the radiation force of the ultrasonic beam exerted on a target is measured. The ultrasonic power is determined by multiplying the velocity of sound in the medium to the measured radiation force. [In distilled water at 20°C, 1-watt power produces approximately

67 mg force (1.3)]. Two different approaches for measuring radiation force have been used (1). In one, the target is suspended and allowed to move under the radiation force. The amount of target movement is measured and converted to force. In the other approach, the force on the target is directly measured using some form of mechanical balance. The target, which must be either totally reflective or totally absorbing, is crucial and thus requires very careful attention in its design and fabrication. To determine the total power of the ultrasonic beam, corrective compensation is needed for the effects of such parameters as attenuation in the medium, spatial variation of beam pattern over the target surface, and reflection coefficient of the target material. Implementation of these techniques, therefore, is somewhat complicated.

In this paper, a simple technique for measuring radiation force, and thus the total acoustic power output, of an ultrasonic transducer is described. The radiation force is measured by weighing the reaction force of the transducer to the transmitted ultrasonic beam. Since no target is used, the technique is easy to implement. Furthermore, because no target-related errors are present, the technique is inherently more accurate than conventional ones.

In the following sections, the underlying principle of the technique and the experimental data obtained with 5-MHz ultrasonic transducers are presented. Next, the advantage of the technique is discussed followed by conclusions.

## REACTION RADIATION-FORCE MEASUREMENT TECHNIQUE

According to Newton's third law of motion, an ultrasonic transducer experiences a reaction force to the radiation force of its transmitted beam. The reaction force is equal in magnitude (and opposite in direction) to the radiation force and can be ascertained using a simple arrangement of a balance beam on a knife edge (seen in Fig. 1).

At one end of the balance beam an ultrasonic transducer is attached and partially immersed in a liquid medium, typically water. The ultrasonic beam when reflected from the bottom of the liquid container is prevented from returning to the transducer by using either an appropriate sound-absorbing material or a beam diverter. Electrical connection to the transducer is made through a thin, flexible wire to remove any interference of the electrical cable with the force measurements. A pointer and a counterweight are attached to the other end of the balance beam. Under the pointer, a precision weighing device is placed to measure the reaction radiation force.

## EXPERIMENT: RESULTS AND DISCUSSION

Using the reaction radiation-force measurement technique and the arrangement shown in Fig. 1, ultrasonic power produced by several 5-MHz transducers was measured at various voltages applied to the transducer. The piezoelectric element of these transducers was made of lead metaniobate and measured 9.5 mm in diameter. The transducers had an epoxy backing and an epoxy matching layer to water load. The impedance of the transducers was approximately 50 ohms at 5 MHz. A 0.015-mm wide and 0.025-mm thick silver ribbon was used as a flexible wire for electrical connection to the transducer. An Arenberg pulsed oscillator (Model PG-650C) served as the ultrasonic instrument, which was operated in a continuous-wave (CW) mode. A digital balance (Ohaus Model Galaxy 120) with a precision of  $\pm 1$  mg functioned as the weighing device. The level of the applied voltage to the transducer was monitored at the location of the thin, flexible wire by applying an oscilloscope probe and displaying the signal on an oscilloscope. To minimize the environmental disturbance such as vibration and air circulation on force measurements, the experimental setup, except the ultrasonic instrument, was placed in an isolation chamber.

The radiation-force measurements were made as follows. First, before energizing the ultrasonic transducer, the counterweight was adjusted so that a bias force was registered on the weighing device. Then, the voltage to the transducer was increased from zero to a selected level by manually adjusting the power output of the ultrasonic instrument. When the applied voltage reached the selected level, the ultrasonic instrument setting was left for about 20 seconds before its power output was reduced back to zero. During this process, the readings of the weighing device were continually recorded and stored in a computer. This process was repeated at various values of the applied voltage.

An example of the data, recorded as a function of time during a measurement process described above, is illustrated in Fig. 2. Initially, no voltage was applied to the transducer, and the weighing device read the bias force. As soon as the transducer was activated by increasing the applied voltage, the readings of the weighing device increased accordingly. When the applied voltage was set to a fixed level, the readings also reached a constant value with a normal fluctuation corresponding to the resolution of the weighing device. When the applied voltage was reduced to zero, the readings returned to the initial bias force. The radiation force of the ultrasonic beam at a specific level of applied voltage was then determined by subtracting the bias force from the data taken at the specified applied voltage.

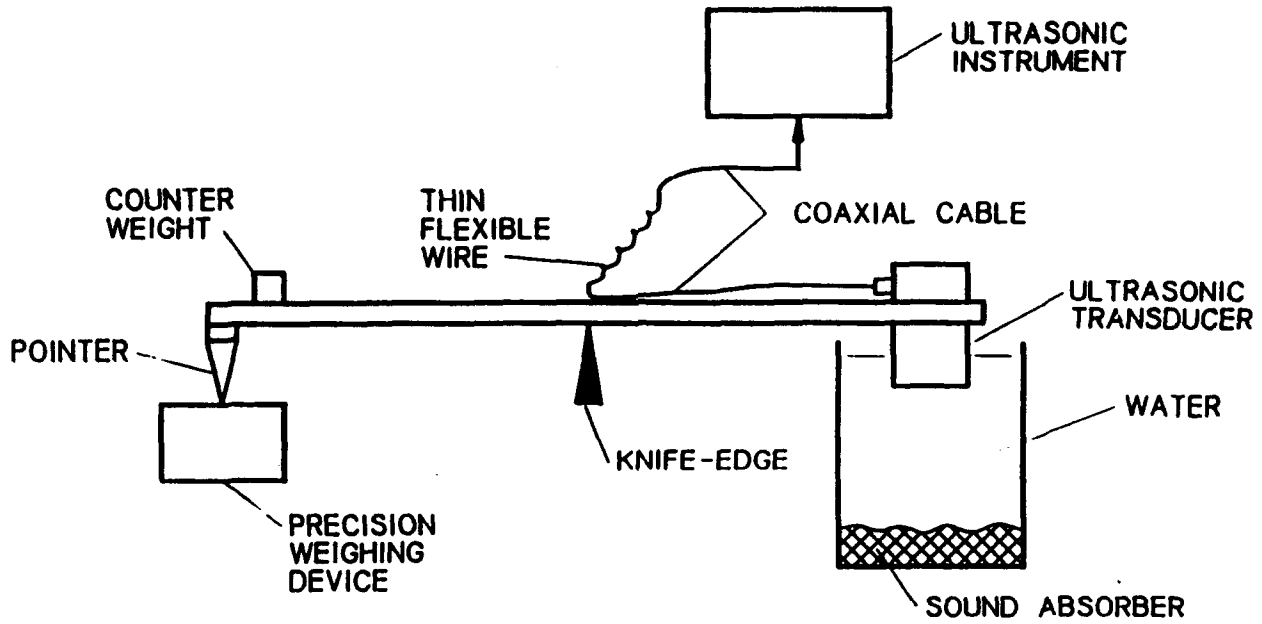


Figure 1. Schematic diagram of an arrangement for measuring ultrasonic power of a transducer using the reaction radiation-force technique

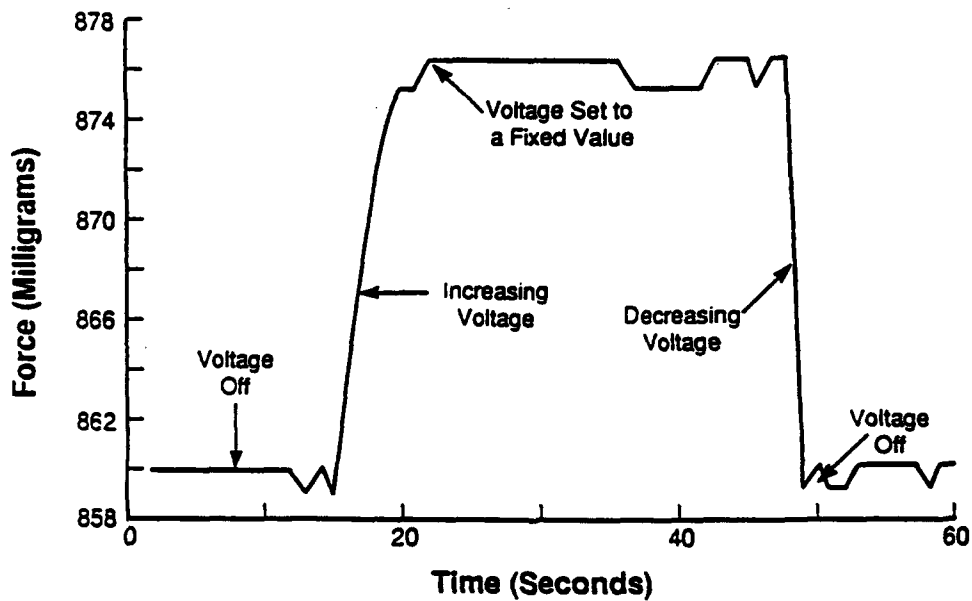


Figure 2. Force as a function of time recorded during a measurement process with a 5-MHz transducer

From the data shown in Fig. 2, it can be observed that the technique and the simple experimental setup readily measured the radiation force of the ultrasonic beam. The sensitivity and stability of the force measurements were  $\pm 1$  mg, which were dictated by the resolution of the Ohaus digital balance used in the experimental setup. Since the reaction radiation-force measurement technique has no inherent limitation, the sensitivity should be improved with the use of a higher resolution weighing device.

The radiation force measured at various values of the applied voltage is plotted in Fig. 3 as a function of the square of the applied voltage. As expected, the measured force was approximately linearly proportional to the square of the applied voltage. The force measurements were reproducible within approximately  $\pm 5$  percent. Most of the measurement error was due to the uncertainty in setting the voltage to the selected level and the instability of the R.F. amplifier of the Arenberg pulsed oscillator, particularly at high levels of the applied voltage. As a result, the least-square-fit line in Fig. 3 does not go through the origin at zero applied voltage.

Excluding the uncertainty in the voltage setting, force measurements with the technique have several potential sources for errors. One is the potential interference of the flexible wire on the mechanical movement of the balance beam. A test with a known weight placed on the transducer indicated that the error was less than  $\pm 1$  percent. Another possible error source is the misalignment of the transducer. Misalignment is estimated as not exceeding 2 degrees; the corresponding error is thus less than  $\pm 0.06$  percent. Another problem could come from wave reflection to the transducer from the water container. A testing of the transducer in a pulse-echo mode showed no significant returning signal, indicating that this error was negligible. Other sources of error including a buoyancy change due to rise in water temperature are also estimated to be insignificant. It is estimated, therefore, that the total error in force measurements for a given applied voltage is about  $\pm 1$  percent.

Because no separate target is used in the reaction radiation-force measurement technique, no target-related errors are present including those caused by uncertainty in the effects of target geometry and by attenuation of the sound beam in the medium. Conversely, for conventional techniques using a target, the uncertainty in attenuation produces a significant measurement error in proportion to the frequency of the ultrasonic beam for frequencies higher than 5 MHz (3). This error makes conventional techniques less reliable at high frequencies. On the other hand, the reaction radiation-force measurement technique should be accurate regardless of the frequency of the ultrasonic beam.

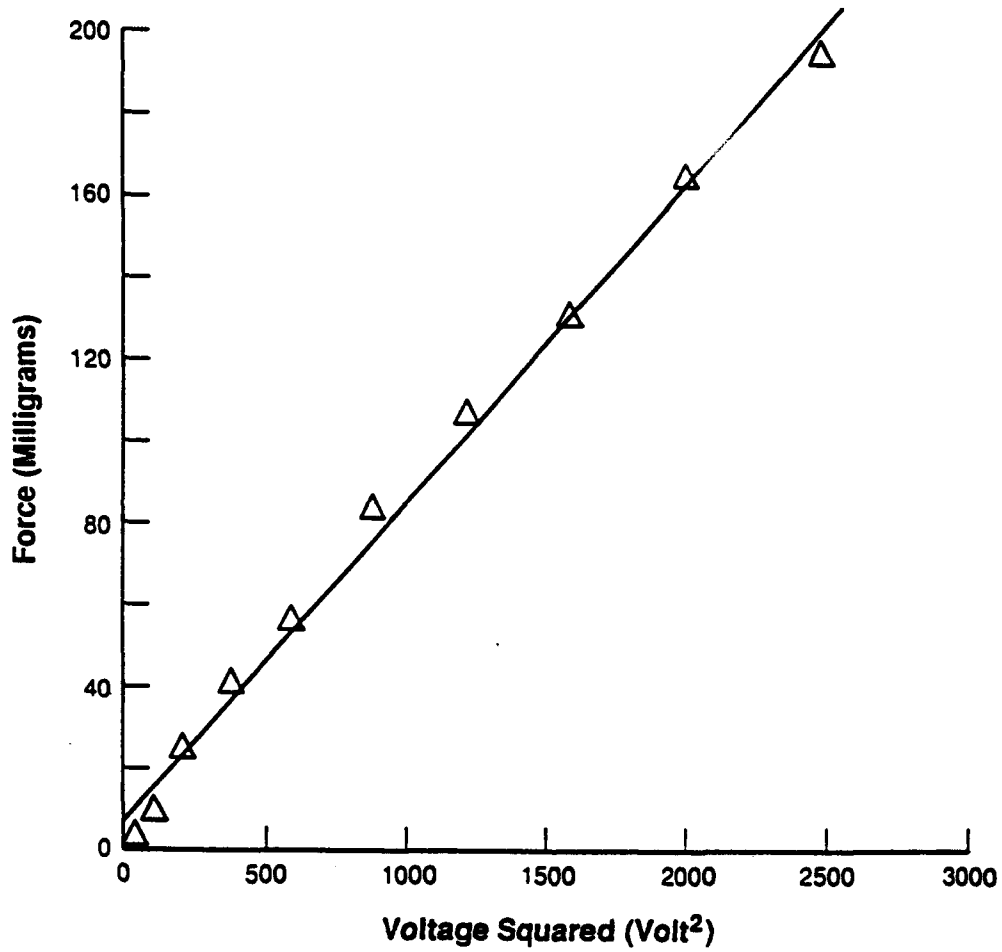


Figure 3. Radiation force vs. square of the applied voltage (obtained from a 5-MHz transducer with voltage in rms)

## CONCLUSIONS

The power of ultrasonic beam was measured using the reaction radiation-force measurement technique. Compared with conventional radiation-force measurement techniques, which use a target, the technique described in this paper is simpler to implement and inherently more accurate.

## ACKNOWLEDGMENTS

This work was supported by U.S. Air Force, School of Aerospace Medicine, Brooks Air Force Base, under contract No. DLA900-84-C-0910, Mod. P00105.

## REFERENCES

1. Zieniuk, J., and Chivers, R. C., "Measurement of ultrasonic exposure with radiation force and thermal methods," Ultrasonics 14 (1976) 161-172 and references therein.
2. Miller, E. B., and Eitzen, D. G., "Ultrasonic transducer characterization at the NBS," IEEE Trans. Sonics and Ultra. SU-26 (1979) 28-37.
3. Greenspan, M., Breckenridge, F. R., and Tschiegg, C. E., "Ultrasonic transducer power output by modulated radiation pressure," J. Acoust. Soc. Am. 63 (1978) 1031-1038.

**APPENDIX B**  
**CIRCUIT DESCRIPTION AND SCHEMATICS**

## DETAILED CIRCUIT DESCRIPTION OF THE PROTOTYPE DOPPLER BUBBLE DETECTOR INSTRUMENT

### 1. Description of System

The specified goal of this development was to produce a pulse-doppler ultrasonic system capable of detecting gas bubbles in blood which is moving at a moderate velocity at depths up to 12 centimeters within the human chest. The development process was one of modifying an existing c.w.-doppler system by adding appropriate timing and gating circuits to achieve a pulsed transmitted signal and a time gated received signal, and an r.f. power amplifier to increase the transmitted ultrasonic power. The rationale for this development was two-fold: it was reasoned that a pulsed transmitted pulse would allow the use of increased transmitted power which would afford greater depth of penetration without exceeding safe time-averaged ultrasonic power levels; and a gated receiver would separate returned signals according to depth of penetration, thus eliminating interference by signals from shallow body structures. In general, the specified goal was achieved; but the decision to use the existing c.w. system as a basis proved to be restrictive relative to achieving the best design from the standpoint of signal-to-noise ratio. The c.w. system is inadequate in two important areas: it does not provide an adequate facility for utilizing time-controlled-gain signals from an external source; and it does not have a proper phase detector for the efficient detection of doppler shifted signals.

### 2. Circuit Description

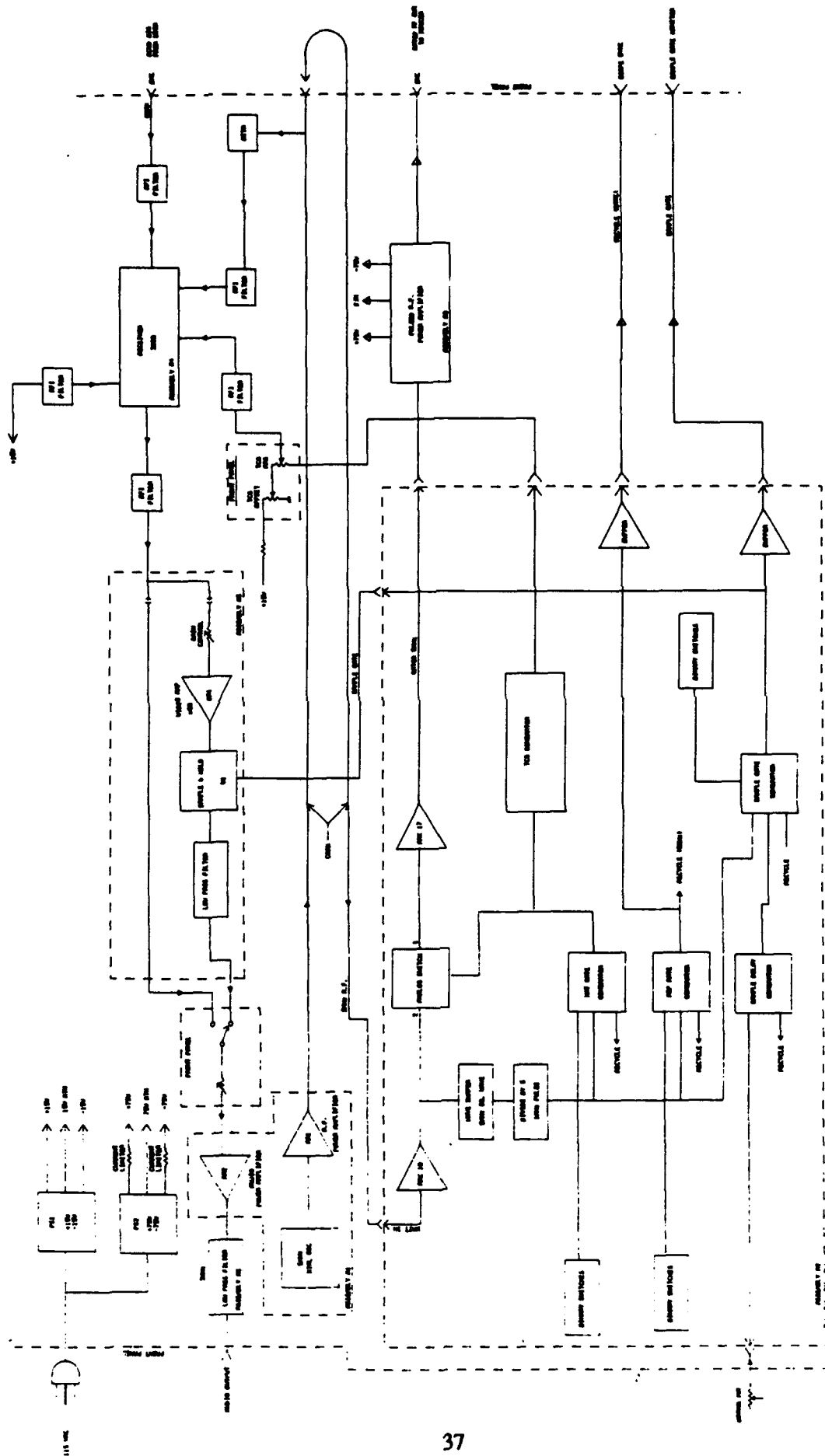
Figure 1 shows a block diagram of the final system design. The system consists of two power supplies and five other circuit assemblies with some additional components included within the inter-assembly wiring and mounted on the main panel.

#### 2.1 *Oscillator*

Tracing a signal through the system, we start with the 5 megahertz crystal controlled oscillator in assembly A1. The output of the oscillator is buffered by an amplifier in A1 and conducted via a coax cable to a BNC connector on the main panel (referred to as the "front panel" on the diagram). The purpose of this connection is to allow for operation in the c.w. mode if desired. A short coax cable extends out of the main panel and, for pulsed-doppler operation, connects to the aforementioned BNC connector, thus leading the 5 MHz. signal back into the system enclosure and terminating at connector J1 of assembly A2.

#### 2.2 *Tone Burst Generator*

On A2, the signal is buffered and input to an analog switch. The switch is turned on and off, by a gating signal from the timing circuits which will be described later, to form at its output a 5 MHz tone burst some 5 to 10 microseconds in duration. The length of the tone burst is precise and adjustable in 1 microsecond increments. The output of the switch is again buffered and led off assembly through connector J2. This tone burst is then amplified as it passes through assembly A3 and on to another BNC on the main panel. At this point the amplitude of the tone burst is approximately 100 volts peak-to-peak. The amplitude is inversely related to the width of the tone burst which tends to keep the average output power relatively constant.



BLACK ENGINEERING- BLACK  
VELOCITY INSTRUMENT  
D-62200

Figure B1. Block Diagram of the Prototype Pulsed Doppler Bubble Detector Instrument

### **2.3 Ultrasonic Doppler Measurement**

From this point, the tone burst is led to the transmitting transducer over a coax cable, the length (up to 20 feet) of which depends on the application configuration. The transducer is coupled to the chest of the person being examined so that the resulting ultrasonic signal is radiated into the chest cavity. Ultrasonic signals of varying magnitudes are returned from the various surface discontinuities within the transmitted beam to a receiving transducer also coupled to the chest. Heart valves and gas bubbles in neighboring blood scatter ultrasonic signals. The movement of these scatterers cause doppler shifts in the scattered signals which can be detected by the system provided the gating of the received signal is properly timed. The apparent magnitude of the received signals depends, among other factors, on how well the "look" volume of the receiving transducer matches the illumination volume of the transmitting transducer.

### **2.4 Ultrasonic Receiver**

The receiving transducer produces electrical analogues of the ultrasonic signals which are conducted over another coax cable to the "RCVD SIG" BNC connector on the main panel. The signal proceeds from this connector through a radio interference (RFI) filter to the input of the receiver assembly A4. In the receiver, the received signal is mixed with a 5 MHz reference signal with the result that the output of the detector contains a beat note the frequency of which equals the doppler shift generated by the pulsating action of the heart valve or by the rushing motion of the blood bubbles. The doppler shift is in the audio range of up to about 5 kilohertz. That is, with proper processing, it produces a signal that can be perceived with the human ear. The processing is outlined in the following paragraphs.

### **2.5 Audio Section**

The output of the detector is filtered and buffered by an amplifier in receiver assembly A4 and conducted over a twisted pair of conductors to the input of the sample and hold assembly A5. The twisted pair passes through an RFI filter before terminating on A5.

### **2.6 Sample-Hold Circuit**

In the sample and hold assembly, A5, the output of the receiver assembly is sampled at a precise delay time interval after the tone burst is output to the transmitting transducer. The sample duration is adjustable, but its optimum value is about 10 microseconds. The sample time and duration are controlled by a pulse from the time generating circuitry on assembly A2. The result of this process is that only signals scattered from a narrow slice of tissue a selected depth in the chest cavity are presented for analysis. What the sample-and-hold circuit does is measure the signal amplitude at a precise time and produce an output level of equal magnitude and will hold that magnitude until the next sample is taken. Without filtering, the output of the sample and hold would look like a series of stair-steps going up and down; but low-pass filtering removes the step-like quality of the signal so that the final output of the sample and hold assembly, A5, is the fluctuation signal that fluctuates in correspondence to the motion of the scatterers in the volume of tissue being interrogated. With proper system adjustments, the volume of interrogation includes high-velocity blood stream immediately following a heart valve with the result that the output of assembly A5 fluctuates very rapidly. Frequency components in the 2 kHz to 4 kHz region would not be uncommon.

## 2.7 Audio Output

The output of the assembly A5 is passed through a switch to a power amplifier and low-pass filter which cuts off rapidly above 4 kHz. The output of the filter is passed to a loudspeaker or earphones so that an operator can listen to and interpret the signals produced by the system.

There are two inputs to the switch following assembly A5: one from the output of the sample and hold assembly, A5, and one directly from the output of the receiver assembly, A4. The switch provides the capability to select either the pulsed-doppler or the c.w. mode of operation. To operate in the c.w. mode, the transmitting transducer has to be connected to the BNC connector that is connected to an r.f. buffer amplifier on assembly A1.

## 2.8 Timing Circuits

The timing circuits for the system are all found on assembly A2. The basic clock for the system is the 5 MHz crystal oscillator on assembly A1. During pulsed-doppler operation, the 5 MHz is input to the assembly A2 via BNC connections on the main panel and J1 on assembly A2. This signal is buffered by an amplifier on A2 and then shaped into a square wave and then its frequency is divided by 5. The output of the divider is a short pulse occurring at a one MHz rate. This signal provides the clock input to all of the counters included in the timing circuits. The re-rate generator is a counter based circuit that produces the "RECYCLE" pulse at a digitally selectable pulse rate. Usually this is set at 6K pps to allow penetration into the chest cavity of about 12 cm. The "RECYCLE" pulse marks the beginning of each new pulsed-doppler acquisition cycle. The "RECYCLE" starts the transmitter gate generator and the sample delay generator.

The transmitter gate generator is a counter-based circuit that generates a pulse of adjustable width. This voltage pulse turns on the switch that controls the time and duration of the transmitted tone burst. The sample delay generator is based on a one-shot multivibrator whose output pulse width is controlled by a panel mounted potentiometer which is connected into the A2 circuitry via connector J1. The delay produced by this circuit is adjustable from 10 to 160 microseconds. At the end of the delay time a short pulse activates the sample gate generator which is counter based and produces an adjustable pulse of about 10 microseconds. The output of this generator is passed to the sample and hold assembly via connector J2 to provide the time and duration control of the sample and hold function. Buffered versions of the "RECYCLE" signal and the sample gate signal are passed to BNC connectors on the main panel to provide synchronization of and a relative timing display on the oscilloscope.

A time-controlled gain (TCG) signal generator is also included on A2. This generator uses the output of the transmitter gate generator to produce a sharply rising pulse that decays exponentially. The output of this circuit is passed to a potentiometer on the main panel which attenuates the signal by an operator selectable amount. The attenuated signal is passed to the receiver assembly, A4, where it operates to quickly reduce the gain of the receiver during the early part of an acquisition cycle and then restore the gain to its full value near the end of an acquisition cycle. There is a second potentiometer on the main panel that is associated with this TCG circuit. This potentiometer is connected to the +15 volt power supply and provides a variable amount of d.c. offset to the TCG signal. This simply adds another degree of variability to the result achieved by the TCG signal.

## **2.9 Power Supplies**

The two illustrated power supplies, PS1 and PS2, provide all of the required d.c. power for the system. Most circuits use the plus and minus 15 volt power. The plus and minus 75 volt power is used only by the power amplifier assembly A3. The two current limiting resistors in series with the outputs of the 75 volt supply serve to protect the power amplifier against over heating in case of some circuit fault. They also act to keep the average output power of the ultrasonic transducer at a safe level regardless of the pulse width.

## **2.10 RFI Filters**

The purpose of the RFI filters in every line connected to the receiver assembly is to prevent the existence of high-frequency ground loops and other interference mechanisms from degrading the operation of the receiver.